MULTI-SENSOR MULTI-SPECTRAL RAIN-RATE RETRIEVAL

A. V. Korpela and M. J. Uddstrom
National Institute of Water and Atmospheric Research
Private Bag 14 901, Wellington, New Zealand

1 INTRODUCTION

The relationship between satellite microwave observations and rain-rate is investigated through analysis of an archive of collocated AMSU (Advanced Microwave Sounder Unit), AVHRR (Advanced Very High Resolution Radiometer), and Doppler weather radar data. The NACA archive (NIWA ATOVS Collocation Archive) was constructed from NOAA-15 AMSU observations collocated with high temporal resolution (15 min) radar data from three New Zealand weather radars, and with visible and near-infrared imager data from AVHRR on NOAA-15 platform. The archive preserves high resolution information at sub-AMSU instantaneous field of view (ifov) scale, allowing to study underlying uncertainties in rain-retrieval algorithms arising from beamfilling effects. Satellite rainfall estimates are of value in nowcasting and rain-process studies, as well as in identifying radiative contaminants in the observations used in numerical weather prediction models (e.g. the New Zealand Limited Area Model, NZLAM-VAR).

2 METHOD

Rain retrieval from AMSU microwave observations can be based on a scattering signal present at AMSU-B high frequency channel. Fig. 1 and Fig. 2 show the different behavior of the brightness temperatures in 89 GHz and 150 GHz channels as a function of ifov mean rain-rate. The brightness temperature has large variation at any given rain-rate, so that the overall rain-signal becomes more apparent after binning, as plotted in the right hand side panels. The average brightness temperature in the longer wavelength 89 GHz channel shows initially rapid increase due to emission from the light rain, and then remains largely constant with increasing rain-rates, whereas in the 150 GHz channel there is a strong monotonic decrease. This is because with higher rain-rates the number of scattering particles comparable to the short wavelength (2 mm) at 150 GHz is higher, and the scattering effect becomes stronger.

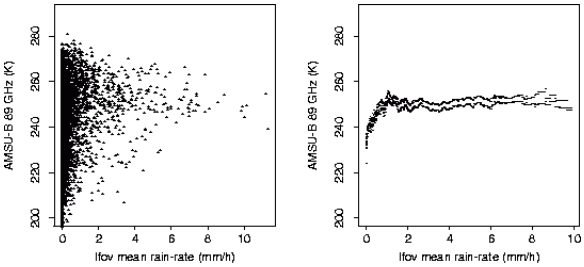

Fig. 1 Brightness temperature signatures of cloud liquid and precipitable water in AMSU-B 89 GHz. Scatter plot (left) and standard error interval of the bin average (right).

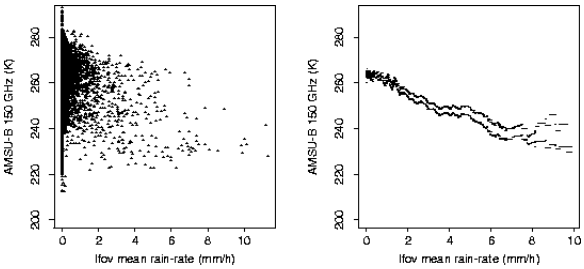

Fig. 2 Brightness temperature signatures of cloud liquid and precipitable water in AMSU-B 150 GHz. Scatter plot (left) and standard error interval of the bin average (right).

We used the NACA AMSU-B database to derive a model for the scatter-free 150 GHz channel brightness temperatures using a subset of cloudy, non-raining over-ocean samples. With negligible scattering on a wide frequency range in these samples, the 89 GHz channel alone is a good predictor for the 150 GHz channel. From the dependent sample set we obtained for the model 150 GHz brightness temperature the expression

Corresponding author address: Aarno V. Korpela, NIWA, Private Bag 14 901, Kilbirnie, Wellington, New Zealand. Email a.korpela@niwa.co.nz

$$T_M(150) = -874.6 + 8.743 \times T_B(89)$$
$$+119.9 \times \cos\theta - 0.01653 \times T_B(89)^2$$
$$-0.4933 \times \cos\theta \times T_B(89)$$

where θ is the local zenith angle of the spacecraft. In raining samples the 89 GHz channel and consequently the derived 150 GHz model remain largely unaffected by the rain. This can be seen in Fig. 3 (left), where the upper plot shows the standard error interval of the model average as a function of ifov mean rain-rate. Compared against this is the measured 150 GHz brightness temperature (repeated from Fig. 2) showing the decrease with increasing rain-rates. The difference between the model and the measured brightness temperature is the scattering index (SI) at 150 GHz, and the standard error interval of its bin average is plotted in Fig. 3 (right).

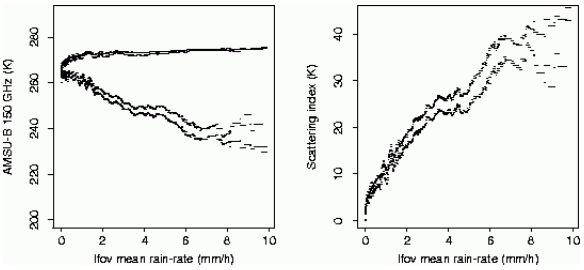

Fig. 3 Left: NACA subset of raining samples. Standard error interval of the bin average of non-precipitating model (upper plot) and measured (lower plot) AMSU-B 150 GHz brightness temperatures. Right: Standard error interval of the bin average of scattering index. Both diagrams plotted against the ifov mean rain-rate.

3 RESULTS

In a general, simple approach to quantify the rainfall, one can take SI as a predictor for the rain-rate regression. It is necessary to limit the samples to those which have high navigation accuracy and have the radar lowest beam distance to bright band (DBB) sufficiently large. In the selected subset the model fit then gave the expression

$$RR(SI) = 0.03746 + 0.03013 \times SI$$
$$+0.001437 \times SI^2$$

for the rain-rate (mmh^{-1}), with explained variance of R^2=0.61.

In order to improve the rainfall estimate from this general model we can use prior knowledge of the rain-processes inside the ifovs. Having SRTex cloud classification done for the ifovs in NACA database, this information can be used to partition the dataset. We derived cloud-class specific rain-rate models RR(SI) for the different cloud-classes by requiring that a large fraction (> 0.90) of the cloudy area in the ifov is filled with the specific cloud. Four cloud-class specific models (for eCu, Ac, Cb, and Cu) performed better than the general RR(SI) model. In the algorithm using cloud classification information, which we will call the SRTex algorithm, we used the RR(SI) models derived from the dependent subset for these four cloud classes. In addition to cloud specific rain models, clouds with none or insignificant rain can be identified, and zero rain-rate estimate assigned, regardless of the scattering index value. Two cloud classes, Sc and St, were defined in this sense as “never raining” in the SRTex algorithm.

The third and final rain-rate algorithm is obtained by combining the SRTex method and the general scattering index relation, so that in those ifovs where the SRTex method can not be applied, the general RR(SI) relation is used instead.

Table 1 summarises the results in terms of the explained variance, when applying the general, SRTex and combined methods to an independent sample set. The table shows the results with three different DBB thresholds. As a graphical example Fig. 4 shows the resulting rain-rate estimate in AMSU-B footprint for the area over New Zealand, when the algorithm is applied to AMSU-B 89 GHz and 150 GHz channels for one NOAA-15 pass in 24th January, 2000.

Table 1 Explained variances and the respective sample sizes of three rain-rate algorithms, when applied to independent cloudy sample sets with three different radar DBB thresholds.

DBB-threshold (km)	General		SRTex		Combined	
	n	R^2	n	R^2	n	R^2
1.0	6654	0.459	4106	0.640	6654	0.510
1.5	2351	0.563	1428	0.691	2351	0.626
2.0	503	0.611	282	0.817	503	0.694

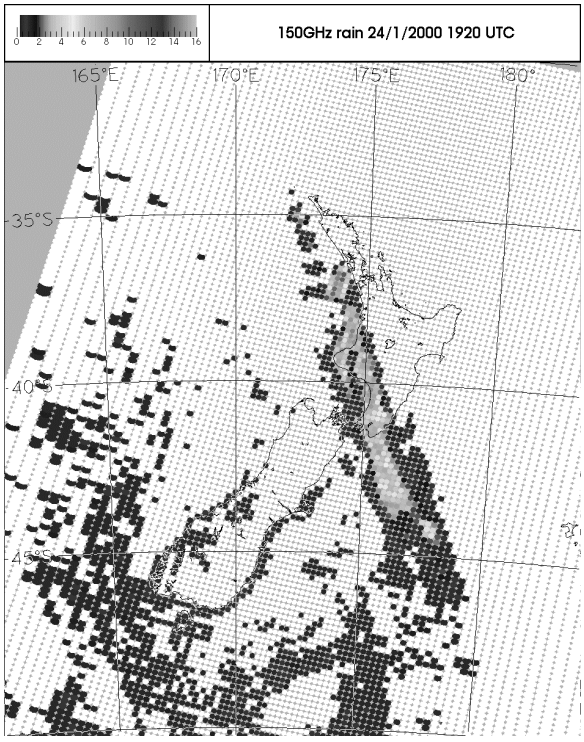

Fig. 4 The RR(SI) scattering index rain-rate algorithm applied to NOAA-15 orbit 8832, 24th January, 2000, 1910-1935 UTC. Mean rain-rate within AMSU-B ifovs.

4 REFERENCES

Bauer, P., P. Amayenc, C.D. Kummerow, E.A. Smith, 2001: Over-Ocean Rainfall Retrieval from Multisensor Data of the Tropical Rainfall Measuring Mission. *Journal of Atmospheric and Oceanic Technology*: **18**, 1838-1855.

Coppens, D., Z.S. Haddad, E. Im, 2000: Estimating the Uncertainty in Passive-Microwave Rain Retrievals. *Journal of Atmospheric and Oceanic Technology,* **17**, 1618-1629.

Ferraro, R.R. and G.F. Marks, 1995: The development of SSM/I rain-rate retrieval algorithms using ground-based radar measurements. *Journal of Atmospheric and Oceanic Technology,* **12**, 755-770.

Grody, N. Weng, F and R.Ferraro, 1999: Application of AMSU for obtaining water vapour, cloud liquid water, precipitation, snow cover and sea ice concentration, In *Technical Proceedings of the Tenth International ATOVS Study Conference,* Boulder, Colorado, USA, 27 Jan. – 2 Feb. 1999. 230 – 240

Morrissey, M.L. and YP Wang, 1995: Verifying satellite microwave rainfall estimates over the open ocean. *Journal of Applied Meteorology,* **34**, 794–804

Kummerow, C., 1998: Beamfilling Errors in Passive Microwave Rainfall Retrievals. *Journal of Applied Meteorology,* **37**, 356–370.

Smith, E.A., J.E. Lamm, R. Adler, J. Alishouse, K. Aonashi, E.Barret, P. Bauer, W. Berg, A. Chang, R. Ferraro, J. Ferriday, S.Goodman, N. Grody, C. Kidd, D. Kniveton, C. Kummerow, G. Liu, F. Marzano, A. Mugnal, W. Olson, G. Petty, A. Shibata, R. Spencer, F. Wentz, T. Wilheit and E. Zipser, 1998: Results of WetNEt PIP-2 Project. *Journal of the Atmospheric Sciences,* **55**, 1483-1536.

Todd, M.C.,C. Kidd, D. Kniveton, T.J. Bellerby, 2001: A Combined Satellite Infrared and Passive Microwave Technique for Estimation of Small-Scale Rainfall. *Journal of Atmospheric and Oceanic Technology,* **18**, 742-755.

Uddstrom, M.J. and W.R. Gray, 1996: Satellite cloud classification and rain-rate estimation using multispectral radiances and measures of spatial texture. *Journal of Applied Meteorology,* **35**, 839-858.